ARTICLE

Determination of Individual Gibbs Energies of Anion Transfer and Excess Gibbs Energies Using an Electrochemical Method Based on Insertion Electrochemistry of Solid Compounds

Antonio Doménech,[*,†] Igor O. Koshevoy,[‡] Noemí Montoya,[§] Antti J. Karttunen,[‡] and Tapani A. Pakkanen[‡]

[†]Departament de Química Analítica, Facultat de Química, Universitat de València, Dr. Moliner 50, 46100 Burjassot, Valencia, Spain
[‡]Department of Chemistry, University of Eastern Finland, FI-80101, Joensuu, Finland
[§]Departament de Química Inorgànica, Facultat de Química, Universitat de València, Dr. Moliner 50, 46100 Burjassot, Valencia, Spain

ABSTRACT: A method is presented to determine, individually and with minimal extra-thermodynamic assumptions, the Gibbs energy for anion transfer between two solvents using solid state electrochemistry of alkynyldiphosphine dinuclear Au(I) complexes $(AuC_2R)_2PPh_2C_6H_4PPh_2$ (**L1**, R = Fc; **L2**, R = C_6H_4Fc) and the heterometallic Au(I)−Cu(I) $[\{Au_3Cu_2(C_2R)_6\}Au_3(PPh_2C_6H_4PPh_2)_3](PF_6)_2$ (**L3**, R = Fc; **L4**, R = C_6H_4Fc) cluster complexes containing ferrocenyl units. These compounds exhibit a well-defined, essentially reversible solid-state oxidation in contact with different electrolytes, based on ferrocenyl-centered oxidation processes involving anion insertion. Voltammetric data can be used for a direct measurement of the free energy of ion transfer from one solvent to another using midpeak potentials in solutions of suitable salts in each one of the solvents separately or mixtures of the solvents. Excess Gibbs energy of solvation in solvent mixtures can also be directly measured using this procedure. Solvation data for different common inorganic oxoanions in water, MeOH, and MeCN and water−MeOH and water−MeCN mixtures are provided.

■ INTRODUCTION

The solvation of ions plays a crucial role in both aqueous and nonaqueous chemistry.[1,2] Similarly, the Gibbs energy of transfer of ions between two solvents and, in particular, between water and different organic liquids is of crucial importance in several fields, from pharmacokinetics to biological ion channels, from solvent extraction techniques to phase transfer catalysis and ion-selective electrodes, among others.[3] Absolute Gibbs free energies of solvation in a given solvent and ion transfer between two solvents can be derived from both computational and experimental studies, but there is a significant uncertainty on the values of such quantity because of the inherent difficulty in its measurement.[4] The reason is that any stable ionic solution contains equal amounts of positive and negative charge, so that experiments can only be performed to determine the sum of solvation free energies of a pair of oppositely charged species. These can be can be determined directly with the aid of thermochemical cycles using calorimetric or electrochemical measurements. Accordingly, additional approximations or models are needed to attribute concrete solvation/transfer free energies to individual ions; that is, such single-ion thermochemical properties can only be evaluated by introducing extra-thermodynamic assumptions.[5−10] Recent theoretical approaches are based on a combination of quantum mechanics calculations to describe the solvent portion in the vicinity of the ion and classical continuum modeling of the solvent relatively far from the ion.[4−14]

The experimental determination of thermochemical properties for single-ion solvation and/or liquid−liquid ion transfer processes involves, in addition to solubility and partition data, electrochemical studies. Recently, several different methodologies

have been proposed involving the direct polarization of liquid−liquid interfaces with two adjacent electrolyte-supported immiscible liquids,[15] membrane-modified liquid−liquid interfaces,[16,17] large surface area,[18] micro/nanohole,[19−22] and triple-phase boundary measurements at microdroplets immobilized on electrode surfaces.[23−26] The application of such methods requires us to establish an universal scale for electrode potentials, provided that the liquid junction potentials, E_{junc}, which arise at the liquid-phase boundaries can be rendered negligible or be estimated reliably in some way.[27] A possibility for doing this is to assume that the liquid junction potentials are negligible when large ions (typically, picrate (Et_4Npic) cells)[28] are used in the salt bridge so that they have similar electrochemical mobilities and (low) solvation Gibbs energies in many solvents.[28,29]

A second approach is based on the assumption that the solvation Gibbs energy of a reference salt composed of a quasi-spherical cation and a quasi-spherical anion of about the same size can be divided equally. Tetraphenylarsonium tetraphenylborate ($AsPh_4BPh_4$, TATB)[30] or tetraphenylphosphonium tetraphenylborate (Ph_4PBPh_4, TPTB)[31] has been recommended as reference salts. A third, extended approach is to use a certain electrochemical couple whose electrode potential is assumed to be solvent-independent. The International Union of Pure and Applied Chemistry (IUPAC) recommended couples include
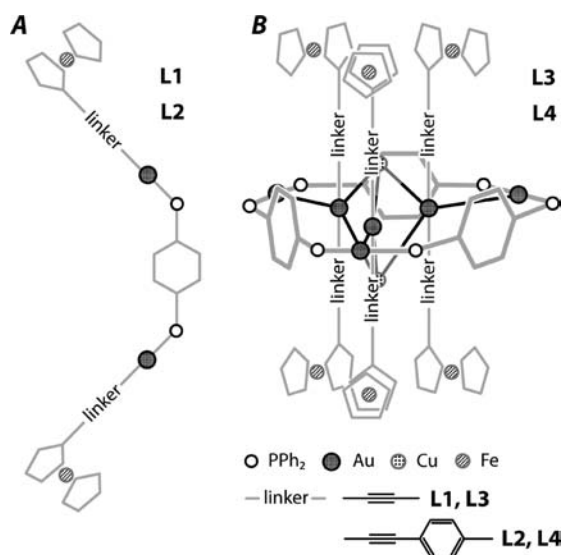
Figure 1. Schematic structures of the complexes **L1** to **L4**. Phenyl rings are omitted for clarity.

ferrocenium/ferrocene $(Fc^+/Fc)^{32}$ or bis(biphenyl)chromium-(I/0) $(BBCr^+/BBCr)^{15,33-36}$ couples.

In this work, it is studied the possibility of using the midpeak potentials obtained in voltammetric experiments for determining individual (rather than ion pair) Gibbs energies for anion transfer between two given solvents and Gibbs energies of excess in solvent mixtures for anions using minimal extra-thermodynamic assumptions. The involved extra-thermodynamic assumptions are: (i) the reference electrode potentials for the two solvents can be related to each other so that the potential of the Fc^+/Fc and $BBCr^+/BBCr$ couples are assumed to be solvent-independent; (ii) there is no accumulation of net charge in the solid complex/electrolyte boundary, (iii) the structure of **L** and anion binding are not affected by the solvent.

For this purpose, the anion-insertion solid-state electrochemistry for a series of recently synthesized[37] alkynyl-diphosphine dinuclear Au(I) complexes $(AuC_2R)_2PPh_2C_6H_4PPh_2$ (**L1**, R = Fc; **L2**, R = C_6H_4Fc) and the heterometallic Au(I)−Cu(I) $[\{Au_3Cu_2(C_2R)_6\}Au_3(PPh_2C_6H_4PPh_2)_3](PF_6)_2$ (**L3**, R = Fc; **L4**, R = C_6H_4Fc) cluster complexes containing ferrocenyl units (see Figure 1) is used. **L1** and **L2** dimers possess a diphosphine unit coordinated to the gold(I) centers, which have the alkynyl ligands functionalized with end-capped ferrocenyl groups as illustrated in Figure 1. **L3** and **L4** are heterotrimetallic clusters whose structure can be described in terms of an alkynyl core $[Au_3Cu_2(C_2R)_6]^-$ "wrapped" by the cationic $[Au_3(PPh_2C_6H_4PPh_2)_3]^{3+}$ "belt", as also illustrated in Figure 1. In the case of Au(I)−Cu(I) alkynyl clusters the alkynyl groups point to the effective communication between the metal core and ancillary ligands, thus favoring electron transfer reactions.[38-41]

Using the voltammetry of microparticles (VMP) approach developed by Scholz et al.,[42,43] such complexes display a reversible oxidation in solid state where the electron transfer process is accompanied by anion insertion.[44] The possibility of using solid-state voltammetry of the studied compounds for potentiostatic and potentiodynamic ions sensing, following the scheme from Bond et al.,[45,46] has been previously explored.[47] In prior works we have applied the VMP methodology to calculate individual Gibbs energies of monovalent anion transfer[48] and cation transfer[49]

between two miscible solvents, in this second case using Prussian blue-modified electrodes. In this report this methodology is extended to a series of bi- and trivalent oxoanions including the estimate of excess Gibbs energies of anion solvation in solvent mixtures and Gibbs energies for anion solvation in water, MeOH, and MeCN. These methods parallel that reported by Scholz et al.[50] for determining Gibbs energies of transfer of ions between two miscible solvents by separate transfer of the ions between each of the solvents and a third phase. Gibbs energies of ion transfer between water/heavy water using a nitrobenzene droplet as the third phase immobilized on the electrode surface have been obtained using this methodology.[50]

Cyclic and square wave voltammetries (CV and SWV, respectively) have been used to study the anion insertion electrochemistry of the studied compounds in contact with aqueous, MeOH, MeCN, and dimethyl sulfoxide (DMSO) solutions of a series of common inorganic oxoanions, namely, ClO_4^-, NO_3^-, HCO_3^-, CO_3^{2-}, SO_4^{2-}, $H_2PO_4^-$, and PO_4^{3-}. The reported methodology allows us to determine, via judicious use of solvent mixtures, the individual (i.e., independent of the counteraction) Gibbs energy of anion transfer even in cases where no available soluble salts exist. The application to the determination of excess free energy of solvation in binary water−MeOH and water−MeCN mixtures is also reported.

EXPERIMENTAL SECTION

Reagents and Equipment. Synthesis and characterization of **L1** to **L4** complexes was performed as previously described.[37] Electrochemical measurements were performed with $(10^{-5}$ to $0.15)$ M aqueous solutions of NaF, NaCl, KCl, NaBr, $LiClO_4$, $NaClO_4$, $LiNO_3$, $NaNO_3$, $NaHCO_3$, Na_2CO_3, KH_2PO_4, Na_3PO_4, and $Na_2SO_4 \cdot 10H_2O$ (all analytical grade Merck reagents), Et_4NCl and Et_4NClO_4, (Aldrich), and Bu_4NClO_4 Bu_4NPF_6 (Fluka) in an electrochemical cell thermostatted at 298 K. Nanopure water, MeOH, MeCN, and DMSO (high-performance liquid chromatography (HPLC) grade reagents, Carlo Erba) were used as solvents. VMP experiments were performed at **L**-modified paraffin-impregnated graphite electrodes (PIGEs, geometrical areas of 0.018 cm^2) using a CH I660 potentiostat. PIGEs were prepared by impregnated pyrolitic graphite bars in vacuo as described in literature.[42,43] A standard three-electrode arrangement was used with a platinum auxiliary electrode and a AgCl (3 M NaCl)/Ag reference electrode, separated from the bulk solution by a salt bridge. Ferrocene (Fluka) was used as an internal standard in the concentration 10^{-4} M.

Electrode Conditioning and Modification. The attachment of the solid complexes **L1** to **L4** to graphite basal electrodes was performed following the procedures recently used by Compton et al.[51] for studying the electrocatalytic performance of carbon nanotubes, based on the mechanical transference of solid microparticles onto inert electrode surfaces. First, ca. 0.5 mg of the complexes were thoroughly powdered in an agate mortar and pestle and extended forming a spot of finely distributed material. Then, the lower end of the graphite electrode was pressed on that spot of the modifier. Second, a film of powdered compounds was formed onto the surface of graphite electrode by pipeting 10 μL of dispersion (1 mg/mL), previously ultrasonicated by 5 min, of the cluster in ethanol and allowing the solvent to evaporate in air. As a result, a uniform, fine coating of the complex was adhered to the basal electrode.
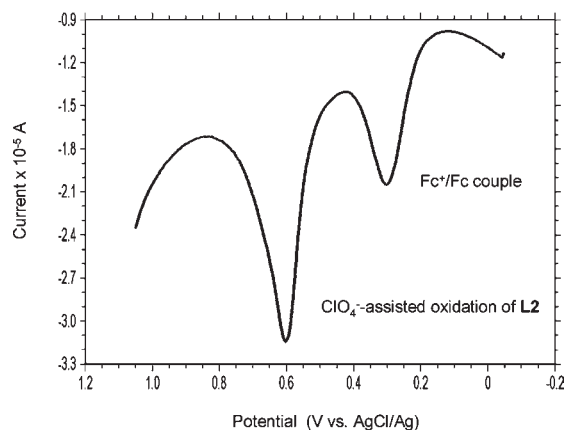
Figure 2. SWV for **L2**-modified PIGE in contact with a 10^{-4} M ferrocene solution in 0.10 M Et_4NClO_4/MeCN plus a 0.10 M $NaClO_4$/water mixture (50:50 v/v). The potential scan was initiated at -0.05 vs AgCl/Ag in the positive direction with a potential step increment of 4 mV, square wave amplitude of 25 mV, and frequency of 5 Hz.

Computational Details. The structural and electronic properties of the ferrocenyl-containing complexes were elucidated by the means of density functional calculations using the BP86 density functional method.[52] The iron, copper, and gold atoms were described with a triple-valence ζ-quality basis set with polarization functions (def2-TZVP),[53] employing a 60-electron relativistic effective core potential for gold.[54] A split-valence basis set with polarization functions on non-hydrogen atoms was used for all of the other atoms (def2-SV(P)).[55] The multipole-accelerated resolution-of-the-identity technique was used to speed up the calculations.[56] All of the electronic structure calculations were carried out with the TURBOMOLE program package (version 5.10).[57]

■ RESULTS AND DISCUSSION

Electrochemical Response. CVs and SWVs for microparticulate deposits of the complexes on graphite in contact with aqueous electrolytes display a one-electron, essentially reversible oxidation process. Similar results were obtained in available nonaqueous media and water—organic solvent mixtures, as shown in Figure 2. Here, the SWV for **L2** in contact with 0.10 M Et_4NClO_4/MeCN plus a 0.10 M $NaClO_4$/water mixture (50:50 v/v) is shown. As can be seen in Figure 2, the well-defined complex-localized oxidation peak is clearly separated from the peak for the oxidation of ferrocene, added in the concentration 10^{-4} M as an internal standard. The anion-assisted oxidation of the complexes satisfies the essential criteria for reversibility: the SWV peak potential (E_p) becomes frequency-independent in the (2 to 500) Hz frequency range, while the midpeak potential (E_{mp}) in CV remains independent of the potential scan rate (in the studied (1 to 500) $mV \cdot s^{-1}$ range). Here, the anodic-to-cathodic peak potential separation tends to be 59 mV at low potential scan rates, as expected for a one-electron reversible process with relatively large ohmic drops.[48] In all cases, in repetitive voltammetry, peak potentials become unchanged after 3 to 5 scans, so that such stationary values were taken for thermochemical calculations. Repeatability tests on series of five freshly prepared electrodes produced standard deviations in midpeak potentials typically between (2 and 5) mV.
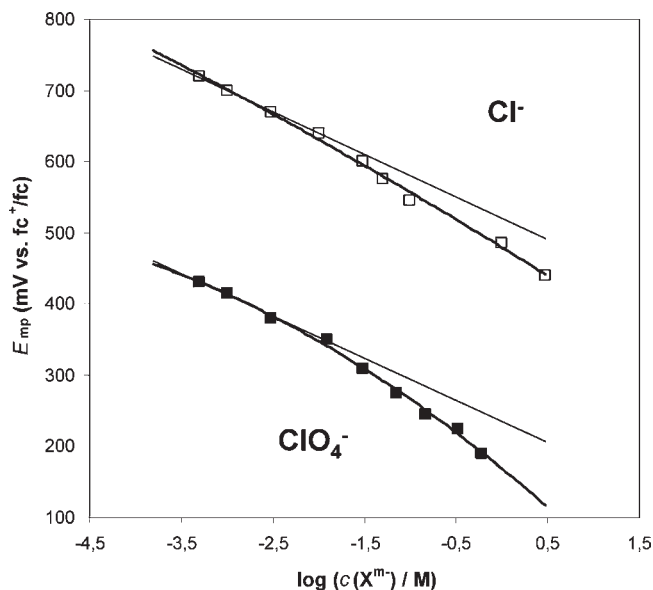
Figure 3. Variation of the midpeak potential determined from cyclic voltammograms (potential scan rate 20 $mV \cdot s^{-1}$) at PIGEs modified with **L1**, on the concentration of NaCl and $NaClO_4$ in water.

The midpeak potentials for the oxidation of **L1** to **L4** complexes in contact with different electrolytes varied from one anion to another while remaining cation-independent, as denoted by experiments using $LiNO_3$ and $NaNO_3$, $LiClO_4$ and $NaClO_4$, and NaCl and KCl in aqueous solvents and experiments using $LiClO_4$, Et_4NClO_4, and Bu_4NClO_4 in both MeOH and MeCN. Consistent with the reversible character of the electrochemical process, E_{mp} versus log(anion concentration) plots were essentially linear in the $(10^{-4}$ to $10^{-2})$ M range, the slope being equal to 59 ± 5 mV. As shown in Figure 3, these plots deviate from linearity at larger anion concentrations. Replacing concentrations by activities using the Davies equation yields essentially linear E_{mp} versus log(anion activity) plots of slope 59 ± 5 mV for all tested anions. In these circumstances the midpeak potential in voltammetric experiments can in principle be taken as a measure of the equilibrium potential of the system and then used for thermochemical measurements, as discussed by Bond et al.[45,46] For thermochemical calculations (vide infra), midpeak potentials at an anion concentration of 10^{-4} M, where it is reasonable to assume that the activity equals the concentration, were taken. Similar results were obtained for experiments in MeOH and MeCN electrolytes. No suitable results were obtained in DMSO because of the solubility of the **L1** to **L4** complexes in this solvent.

The observed electrochemistry can be described on the basis of the theoretical modeling for solid-state electrochemical reactions[58−63] based on the idea that the electrochemical process is initiated at the particle/electrode/electrolyte three-phase boundary, further expanding over the surface and into the body of the solid particle. Charge transport occurs via electron hopping between adjacent immobile redox centers in the solid coupled with ion transport through the solid so that electron and ion diffusion take place in mutually perpendicular directions through the solid particles.

According to this formulation, the solid-state voltammetric response observed for complex-modified electrodes can be described in terms of the essentially reversible, anion-assisted oxidation of the ferrocenyl units of the **L** complexes. For both

Table 1. HOMO/LUMO Energies Respective to the Vacuum Level Calculated for Complexes L1 to L4

	L1	L2	L3	L4
E_{HOMO} (eV)	−4.039	−4.191	−7.131	−6.747
E_{LUMO} (eV)	−2.698	−2.726	−5.821	−5.721
band gap (eV)	1.34	1.46	1.31	1.03

neutral complexes **L1** and **L2** and ionic complexes **L3** and **L4** (all represented as L), the oxidation process can be represented as:

$$\{L\} + (n/m)Y^{m-}(solv) \rightarrow \{L^{n+} \cdots (n/m)Y^{m-}\} + ne^- \tag{1}$$
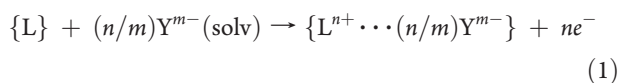
where {} denotes solid phases and (solv) solvated species in solution phase. Evidence for the occurrence of anion insertion processes was provided by chronoamperometric data and scanning electrochemical microscopy/energy dispersive X-ray analysis of microparticulate deposits submitted to controlled potential coulometry in contact with different aqueous electrolytes, as already reported.[44,48]

Correlation of Electrochemical Data with HOMO/LUMO Calculations. Electrochemistry can be correlated with a theoretical quantum mechanics calculation for the energies of the highest occupied molecular orbital (HOMO) and lowest unoccupied molecular orbital (LUMO) used to describe isolated complexes. It should be noted that there is a problem of correlating HOMO/LUMO energies and of the respective spectroscopic data with electrochemistry, because in electrochemistry there is always the contribution from the ion transfer, which is not the case in spectroscopy when electrons are only going from the LUMO to the HOMO, but with the overall charge state being unchanged. Several attempts to approximately describe the relationship between W_{HOMO} determined from ultraviolet photoemission spectroscopy (UPS) experiments and electrode potentials have been reported.[64,65] The recent formulation due to D'Andrade et al.[66] for thin solid films deposited on electrodes assumes that W_{HOMO} can be taken as the energy required to singly ionize a molecule in the solid, now regarded as a homogeneous medium of relative dielectric constant ε_{sol}. The polarizable ion is approximated as a dipole molecule consisting of a positive core surrounded by an electron cloud of effective radius R, so that the HOMO energy (as measured by UPS experiments) can in principle approach the electrostatic energy of the ion−electrode system considering image charge effects. Equating the potential of a conducting surface at the points nearest and farthest from the electrode, the molecular potential, as measured by its oxidation voltage (given by E_{mp} in voltammetric experiments), will be linearly dependent on W_{HOMO}:

$$E_{mp} = E_{vac} + \frac{W_{HOMO}}{eFs} \tag{2}$$

In this equation, s is a factor depending on the ion radius and dielectric constant of the film and the effective dielectric constant near the electrode, which is a function of both the dielectric constant of the solvent and the screening from the electrolyte. The term E_{vac} is introduced to account for the correlation between the vacuum energy scale used in HOMO/LUMO computations, and the standard hydrogen electrode (SHE) scale used for electrode potentials.
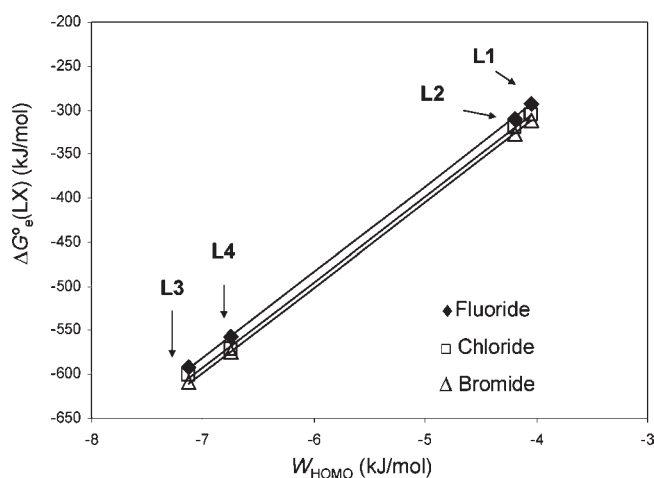

Figure 4. Plots of $\Delta G°_e(LX)$ vs W_{HOMO} for the solid state oxidation of complexes **L1** to **L4** in contact with fluoride, chloride, and bromide aqueous solutions. $\Delta G°_e(LX)$ values are calculated as nFE_{mp} from the experimental midpoint potentials and theoretical W_{HOMO} values from density functional calculations.
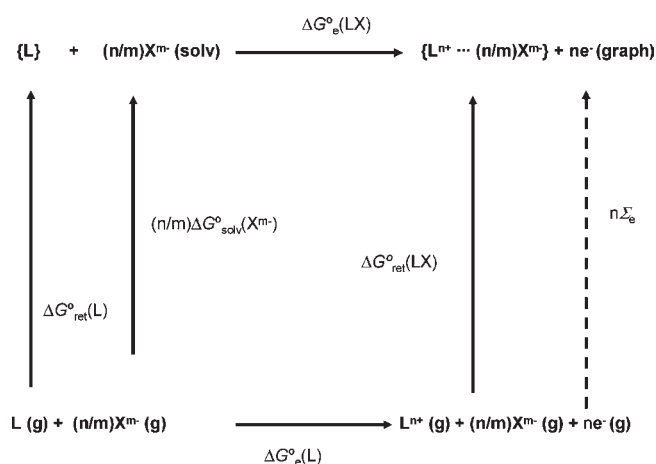
Figure 5. Thermochemical cycle used to describe the anion-assisted oxidation of the studied complexes when both the oxidized and the reduced forms of the complex are insoluble in the solvent.

The HOMO/LUMO energies calculated from density functional calculations for complexes **L1** to **L4** are summarized in Table 1. Introducing the free energy for the electrochemical oxidation process described by eq 1, $\Delta G°_e(LX)$, as nFE_{mp}, plots of $\Delta G°_e(LX)$ versus W_{HOMO} should be linear. Data for the solid state oxidation of complexes **L1** to **L4** are in agreement with this assumption, as can be seen in Figure 4 for complex-modified electrodes in contact with fluoride, chloride, and bromide aqueous solutions.

Thermochemistry of Ion Transfer. To extract thermochemical information on anion solvation from voltammetric data, the electrochemical processes described by eq 1 can be written as a thermochemical cycle such as that represented in Figure 5. The variation of Gibbs energy associated with the electrochemical oxidation of the parent complex, $\Delta G°_e(LX)$, is related to the corresponding quantity for the complex in the gas phase, $\Delta G°_e$-(L), the Gibbs energy of anion solvation/hydration, $\Delta G°_{solv}$-(X^{m-}), and the Gibbs energies for the formation of the parent

4580

dx.doi.org/10.1021/je200514c |*J. Chem. Eng. Data* 2011, 56, 4577–4586
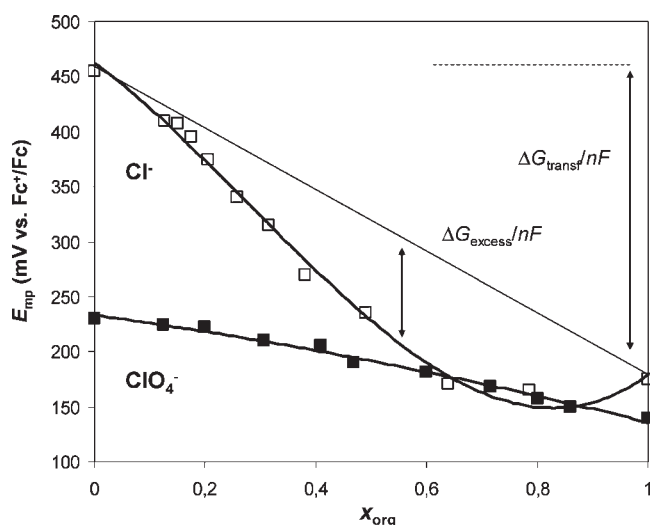
Figure 6. Variation with the molar fraction of organic solvent of the SWV peak potentials for **L1**-modified graphite electrodes immersed into 0.10 M Et$_4$NCl/MeOH + 0.10 M NaCl/H$_2$O (open squares) and 0.10 M LiClO$_4$/MeOH + 0.10 M LiClO$_4$/H$_2$O (solid squares) mixtures. Curves represent the best polynomial fit of experimental data, with a potential step increment of 4 mV, square wave amplitude of 25 mV, and frequency of 5 Hz.

complex and its oxidized form from the ionic species in gas phase, the anion-containing complex, $\Delta G°_{ret}(L)$ and $\Delta G°_{ret}(LX)$, respectively. Upon generalization for X^{m-} anions, the above thermochemical cycle leads to the relationship:[48]

$$\Delta G°_e(LX) = \Delta G°_e(L) + G°_{ret}(LX) - \Delta G°_{ret}(L) \\ - (n/m)\Delta G°_{solv}(X^{m-}) + n\Sigma_e \tag{3}$$

with Σ_e being the free energy for the transfer of one electron from the vacuum to the graphite electrode.

If the voltammetric experiment is repeated for microparticulate deposits of the complexes in contact with a second solvent where the complexes remain insoluble, the thermochemical cycle and eq 3 remain still valid merely by replacing the Gibbs energy for anion solvation in the first solvent, $\Delta G°_{s1}(X^{m-})$, by the Gibbs energy of anion solvation in the second solvent, $\Delta G°_{s2}(X^{m-})$. Then, the Gibbs energy for the transfer of the anion from the solvent s1 to the solvent s2, $\Delta G°_{1\rightarrow2}(X^{m-})$, can be calculated as the difference between the free energies for the X^{m-}-assisted electrochemical oxidation of **L** in the solvent s1, $\Delta G°_e(LX)^{s1}$ and in the solvent s2, $\Delta G°_e(LX)^{s2}$, as:

$$\Delta G°_{s1\rightarrow s2}(X^{m-}) = \Delta G°_{s2}(X^{m-}) - \Delta G°_{s1}(X^{m-}) \\ = (m/n)[\Delta G°_e(LX)^{s1} - \Delta G°_e(LX)^{s2}] \tag{4}$$

Assuming Nernstian behavior, $\Delta G°_e(LX)$, corresponding to the oxidation process described by eq 1, equals nFE_{mp}, so that:

$$\Delta G°_{w\rightarrow s}(X^{m-}) = mF[E_{mp}^{s1} - E_{mp}^{s2}] \tag{5}$$

E_{mp}^{s1} and E_{mp}^{s2} being, respectively, the voltammetric midpeak potentials recorded in the solvents 1 and 2. Accordingly, the $\Delta G°_{1\rightarrow2}(X^{m-})$ values for the anion transfer from water to a given organic solvent can be calculated, using eq 5, from the midpeak potentials extrapolated at 10^{-4} M concentration in solutions of

electrolytes containing the X^{m-} anion in the different solvents, separately. In most cases, however, there are no disposable salts soluble in both solvents. To avoid this problem, a second approach, involving the use of solvent mixtures, can be used. Figure 6 shows the variation with the molar fraction of organic solvent of the SWV peak potentials for **L1**-modified graphite electrodes in contact with 0.10 M Et$_4$NCl/MeOH + 0.10 M NaCl/H$_2$O and 0.10 M LiClO$_4$/MeOH + 0.10 M LiClO$_4$/H$_2$O mixtures. In these cases, the variation of E_{mp} on the molar fraction of organic solvent, x_{org}, can satisfactorily be fitted to a polynomial curve, as can be seen in Table 2, where the statistical parameters for selected polynomial fits in MeOH are listed. As depicted in Figure 6, the E_{mp}^{org} values can be obtained upon extrapolation of the above curves to $x_{org} = 1$ using the above polynomial fits.

In several cases, however, there is an abrupt change in the voltammetric response so that, from a given threshold value of x_{org}, the midpeak potential become constant, $E_{mp}*$. Remarkably, this value is identical for all of the anions displaying the aforementioned behavior. This can be seen in Figure 7, where the variation of the peak potential in SWVs of **L1**-modified electrodes in contact with Na$_2$SO$_4$/(water + MeCN) and KH$_2$PO$_4$/(water + MeCN) mixtures with the molar fraction of organic solvent is shown. These features can be interpreted as the result of the solubility of the oxidized $\{L^{n+}\cdots(n/m)X^{m-}\}$ species. Then, the electrochemical process should be described as:

$$\{L\} \rightarrow L^{n+}(solv) + ne^- \tag{6}$$

The variation of Gibbs energy for this process, $\Delta G°_e(LX)*$, can be related with $\Delta G°_e(L)$, the reticular Gibbs energy of the parent complex, Σ_e, and the Gibbs energy of L^{n+} solvation (see Figure 8). These quantities are related by the relationship:

$$\Delta G°_e(LX)* = \Delta G°_e(L) - \Delta G°_{ret}(L) \\ + \Delta G°_{solv}(L^{n+}) + n\Sigma_e \tag{7}$$

Combining, as before, the expressions for two different solvents, the Gibbs energy for the transfer of L^{n+} from 1 to 2, $\Delta G°_{s1\rightarrow s2}(L^{n+})$, will be given by:

$$\Delta G°_{s1\rightarrow s2}(L^{n+}) = [\Delta G°_e(LX)*^{s2} - \Delta G°_e(LX)*^{s1}] \\ = nF(E_{mp}^{s2} - E_{mp}^{s1}) \tag{8}$$

Experimental data lead to $\Delta G°_{s1\rightarrow s2}(L^{n+})$ for the transfer from MeOH to MeCN of −2.4 (**L1**), +1.0 (**L2**), −8.7 (**L3**), and −2.9 kJ·mol^{-1} (**L4**).

To calculate the Gibbs energy of anion transfer from water to MeOH and MeCN, the E_{mp}^w and E_{mp}^{org} values determined from voltammetric experiments were used. Following the IUPAC recommendations,[32−36] it will be assumed that the potential of the bis(biphenyl)chromium(I)/bis(biphenyl)chromium(0) (BBCr$^+$/BBCr) couple is solvent-independent. Accordingly, the experimental potentials relative to the AgCl/Ag reference electrode must be converted into potentials relative to the BBCr$^+$/BBCr electrode taking the potential of the AgCl/Ag relative to BBCr$^+$/BBCr equal to (+780, +330, and +350) mV in water, MeOH, and MeCN, respectively.[34]

Using this methodology, an excellent agreement was obtained for each anion using different electrolytes and complexes, as illustrated in Table 3, where the values for Gibbs free energy of ion transfer from water to MeCN obtained for the ClO$_4^-$ ion using **L1**- to **L3**-modified electrodes immersed in Bu$_4$NClO$_4$,

Table 2. Statistical Parameters for Polynomial Fit of E_{mp} vs x ($= x_{org}$) Curves for the Studied Anions in MeOH−Water Mixtures[a]

anion	solvents	x_{org} interval	equation
Cl^-	water−MeOH	$0 < x < 0.525$	$E_{mp} = 464x^3 - 347x^2 - 403x + 464$ ($r = 0.998$)
ClO_4^-	water−MeOH	$0 < x < 1$	$E_{mp} = 84x^3 - 153x^2 - 22x + 230$ ($r = 0.9990$)

[a] Peak potentials in mV obtained from SWVs at **L2**-modified electrodes immersed into 0.10 M NaCl/water + 0.10 M Et_4NCl/MeOH and 0.10 M LiClO$_4$/water + 0.10 M LiClO$_4$/MeOH. Potential in mV vs Fc$^+$/Fc.
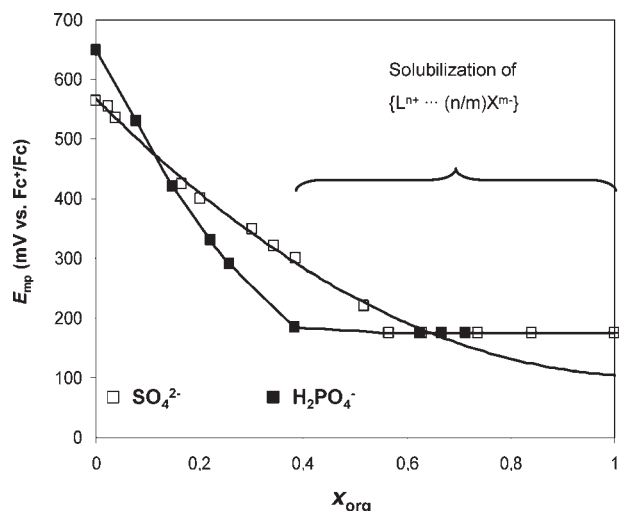
Figure 7. Variation of the peak potential in SWVs of **L1**-modified electrodes in contact with Na$_2$SO$_4$/(water + MeCN) and KH$_2$PO$_4$/(water + MeCN) mixtures (total concentration of the anion 0.10 M). Curves represent the best polynomial fit of experimental data with a potential step increment of 4 mV, square wave amplitude of 25 mV, and frequency of 5 Hz.
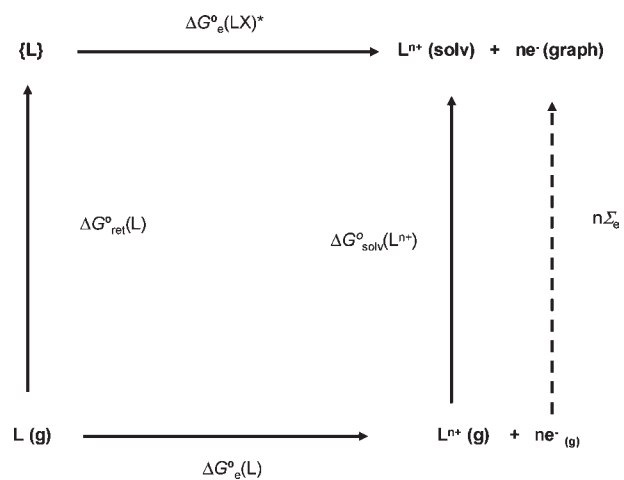
Figure 8. Thermochemical cycle used to describe the oxidation of the studied complexes when the reduced form is insoluble, while the oxidized form is soluble in the solvent.

Et$_4$NClO$_4$, LiClO$_4$, and NaClO$_4$ electrolytes are summarized. Using the E_{mp}^{w} or E_{mp}^{solv} values relative to the BBCr$^+$/BBCr couple, the Gibbs energy of ion transfer from water to MeOH and MeCN was estimated for tested anions. The obtained values are summarized in Table 4, where the average values calculated from data at **L1** to **L4** complexes for MeOH, and **L1** to **L3** complexes for MeCN are reported and compared with literature

Table 3. Free Energy of Ion Transfer from Water to MeCN ($\Delta G°_{w \rightarrow s}$, kJ·mol^{-1}) Obtained for the ClO$_4^-$ Ion Using L1 to L3-Modified Electrodes Immersed in Different Electrolytes[a]

electrolyte	**L1**	**L2**	**L3**
Et$_4$NClO$_4$	6.2 ± 0.2	7.0 ± 0.4	7.0 ± 0.4
Bu$_4$NClO$_4$	6.4 ± 0.2	6.6 ± 0.2	6.2 ± 0.3
LiClO$_4$	7.3 ± 0.3	7.2 ± 0.4	6.8 ± 0.4
NaClO$_4$	6.8 ± 0.4	7.6 ± 0.4	7.3 ± 0.4

[a] From CVs at MeCN−water mixtures containing the electrolyte in a 0.10 M concentration.

Table 4. Free Energy of Anion Transfer from Water to MeOH and MeCN[a]

anion	$\Delta G°_t(w \rightarrow MeOH)$	$\Delta G°_t(w \rightarrow MeCN)$
F$^-$	26 ± 2[b]	65 ± 5[b]
Cl$^-$	13.5 ± 1.2[b] (12.5;[c] 13.7[d])	36 ± 2[b] (37.6;[c] 31.4[d])
Br$^-$	11.5 ± 1.5[b] (10.4;[c] 11.4[d])	36 ± 2[b] (37.6;[c] 31.4[d])
NO$_3^-$	2.0 ± 0.5[b]	12.0 ± 0.6[b]
ClO$_4^-$	5.8 ± 0.2[b] (5.7[d])	7.2 ± 0.4[b] (4.0[d])
SO$_4^{2-}$	36 ± 2[b]	52 ± 3[b]
HCO$_3^-$	21 ± 1[b]	32 ± 2[b]
CO$_3^{2-}$	41 ± 3[b]	126 ± 12[b]
H$_2$PO$_4^-$	29 ± 3[b]	
PO$_4^{3-}$	158 ± 12[b]	

[a] Average values in kJ·mol^{-1} from experimental data at **L1**- to **L4**-modified electrodes immersed into different electrolytes. [b] This work. [c] From Kelly et al.[4] [d] From Cox and Waghorne.[67]

data.[4,67] A satisfactory agreement was obtained between the $\Delta G°_t$ calculated here and those reported in literature although, obviously, in the cases of limited solubility of the electrolyte, the uncertainty of the free energies estimated here is relatively high. In spite of this, the obtained $\Delta G°_t$ and $\Delta G°_{solv}$ (vide infra) values fall within the range of literature values, where discrepancies until ca. 10 kJ·mol^{-1} exist for values calculated by different sources.[4−7,67,68]

To obtain the free energy of ion solvation in a given solvent, the above $\Delta G°_t$ values can be combined with available $\Delta G°_{solv}$ values to obtain the corresponding anion solvation Gibbs energy in the problem solvent. Interestingly, the values of the midpeak potentials or, equivalently, the corresponding difference $\Delta G°_e$-(LX) − $\Delta G°_e$(L) can be correlated with the free energy of solvation, $\Delta G°_{solv}(X^{m-})$ for a given anion in a given solvent. As previously described,[48] such plots can be used for estimating the Gibbs energy of solvation of anions like PF$_6^-$ for which there is no disposal of salts suitable for experiments in aqueous solution. Table 5 summarizes the $\Delta G°_{solv}(X^{m-})$ values estimated for the studied anions from our $\Delta G°_{w \rightarrow s}(X^{m-})$ values obtained from electrochemical data. In view of the high solubility of $\{L^{n+} \cdots (n/m)X^{m-}\}$

Table 5. Free Energy of Anion Solvation in MeOH and MeCN Calculated from Experimental Free Energies for Anion Transfer and $\Delta G^{\circ}_{hyd}(X^{m-})$ in Reference 68[a]

| anion	$\Delta G^{\circ}_{hyd}(X^{m-})$	$\Delta G^{\circ}_{solv}(X^{m-})^{MeOH}$	$\Delta G^{\circ}_{solv}(X^{m-})^{MeCN}$
F^-	-465^b	-439^c	-400^c
Cl^-	-340^b	-327^c	-295^c
Br^-	-315^b	-303^c	-279^c
NO_3^-	-300^b	-298^c	-288^c
ClO_4^-	-205^b	-198^c	-198^c
SO_4^{2-}	-1080^b	-1044^c	-1028^c
HCO_3^-	-335^b	-314^c	-303^c
CO_3^{2-}	-1315^b	-1274^c	-1189^c
$H_2PO_4^-$	-465^b	-436^c	
PO_4^{3-}	-2765^b	-2607^c	

[a] Average values in kJ·mol^{-1} from experimental data at **L1**- to **L4**-modified electrodes immersed into different electrolytes. [b] From Moyer and Bonnesen.[68] [c] This work.
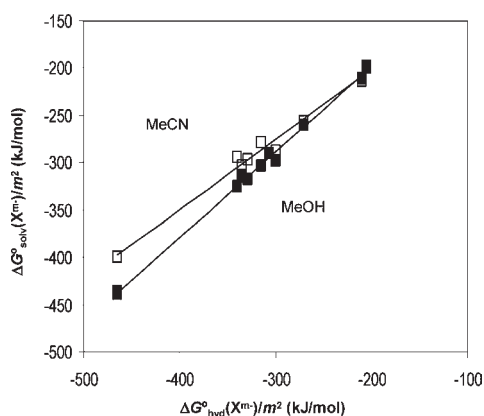
Figure 9. Plots of $\Delta G^{\circ}_{solv}(X^{m-})/m^2$ ratios for MeOH and MeCN vs the $\Delta G^{\circ}_{hyd}(X^{m-})/m^2$ ratio using data in Table 5 and previously reported values.[48]

for phosphate-type ions in MeCN−water mixtures (see Figure 7), no estimates of $\Delta G^{\circ}_{w \to s}(X^{m-})$ were made for $H_2PO_4^-$ and PO_4^{3-} anions. To use a consistent series of Gibbs energy of hydration, the $\Delta G^{\circ}_{hyd}(X^{m-})$ values tabulated by Moyer and Bonnesen[68] have been taken. As indicative of the self-consistency of the obtained results, the calculated values of $\Delta G^{\circ}_{solv}(X^{m-})$ in MeOH and MeCN present an excellent correlation with the $\Delta G^{\circ}_{hyd}(X^{m-})$ values, as can be seen in Figure 9, where the $\Delta G^{\circ}_{solv}(X^{m-})/m^2$ ratios for MeOH and MeCN are plotted versus the $\Delta G^{\circ}_{hyd}(X^{m-})/m^2$ ratio using data in Table 5 and previously reported values.[48] The use of such ratios is derived from the well-known Born expression for the Gibbs energy of ion solvation.[1,2]

Excess Gibbs Energies in Solvent Mixtures. As previously noted, the voltammetric response of **L1** to **L4** complexes in contact with MeOH + water and MeCN + water mixtures was in general qualitatively identical to that obtained in pure solvents. In several few cases, the voltammetric response was complicated by the appearance of peak splitting. This is the case of $NaNO_3$ in water + MeCN solutions depicted in Figure 10. As can be seen in this figure, at molar fractions of MeCN ca. 0.25, two overlapping voltammetric peaks appear, both being shifted upon varying the molar fraction of organic solvent.
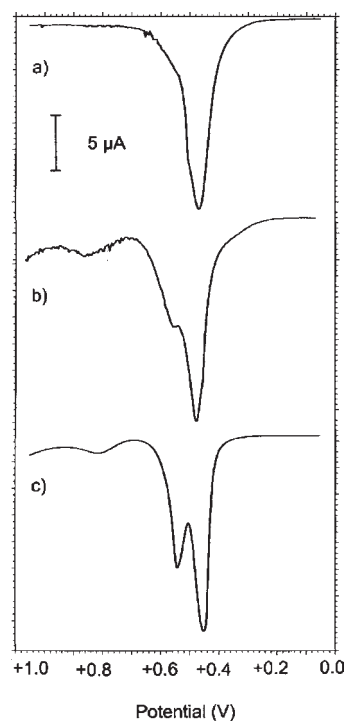

Figure 10. Square wave voltammograms for **L1**-modified PIGEs immersed into 0.10 M $NaNO_3$ water + MeCN mixtures with (a) $x_{MeCN} = 0.054$; (b) $x_{MeCN} = 0.126$; (c) $x_{MeCN} = 0.255$. The potential scan was initiated at +0.05 V in the positive direction with a potential step increment of 4 mV, square wave amplitude of 25 mV, and frequency of 5 Hz.

This response can be rationalized on considering that ion solvation in a mixture of two solvents can be modeled in at least two extreme forms: (i) as mixed solvation, so that a progressive, "smooth" replacement of the molecules of the first solvent by the molecules of the second occurs in the coordination sphere of the ion when the proportion of the second solvent is increased, and (ii) as separate-like solvation, where the ion forms different solvates where the coordination sphere is formed exclusively (or predominantly) by each one of the solvents.[69−74]

Peak splitting appearing in several solvent mixtures can in principle be attributed to kinetic aspects associated to the electrochemical process described by eq 1. These kinetic complications can tentatively be assigned to desolvation processes preceding the ingress of the anions into the solid complexes, as suggested by comparison with theory for the SWV of surface electrode reaction coupled with preceding chemical reaction.[75] The possibility of acquiring information on the structure of the solvated species from this kind of electrochemical data will be subject for future research.

In the absence of peak splitting, voltammetric data at **L**-modified electrodes can be used for determining the free energy of ion solvation in binary solvent mixtures and the excess free energy of ion solvation, $\Delta G^{\circ}_{excess}(X^{m-})$. This can be estimated as the deviation from the actual $\Delta G^{\circ}_{solv}(X^m)$, determined from voltammetric data for a given composition of the solvent mixture, and the "ideal" free energy of solvation, $\Delta G^{\circ}_{solv}(X^{m-})^*$, calculated as the weighted contribution of the two solvents. For

4583

dx.doi.org/10.1021/je200514c |*J. Chem. Eng. Data* 2011, 56, 4577–4586
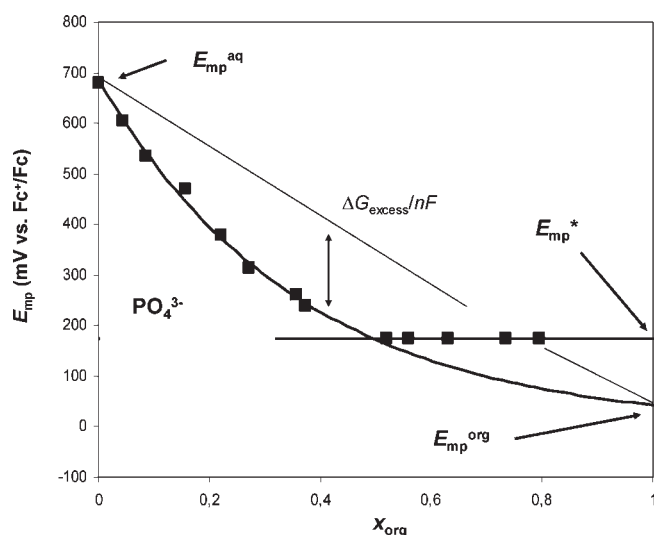
Figure 11. Variation with the molar fraction of MeOH of the SWV peak potentials for **L1**-modified graphite electrodes immersed into 0.10 M Na_3PO_4/(water + MeOH) mixtures. Curves represent the best polynomial fit of experimental data with a potential step increment of 4 mV, square wave amplitude of 25 mV, and frequency of 5 Hz.
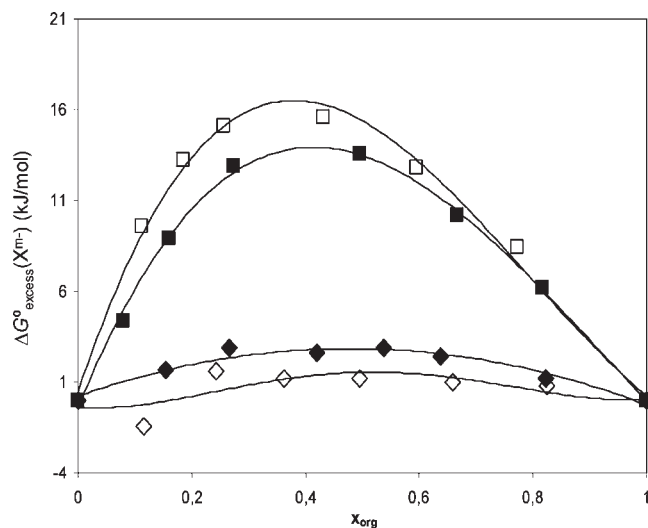
Figure 12. Excess Gibbs free energy of solvation calculated from electrochemical data for perchlorate and acetate ions in 0.10 M $LiClO_4$/MeOH + 0.10 M $LiClO_4$/H_2O (solid diamonds), 0.10 M $LiClO_4$/MeCN + 0.10 M $LiClO_4$/H_2O (open diamonds), 0.10 M Bu_4NAcO/MeOH + 0.10 M $NaAcO$/H_2O (solid squares), and 0.10 M Bu_4NAcO/MeCN + 0.10 M $NaAcO$/H_2O (open squares) binary mixtures. Curves represent the best fit of experimental data.

water–organic solvent mixtures, this can be written as:

$$\Delta G^\circ_{excess}(X^{m-})* = x_{org}\Delta G^\circ_{solv}(X^{m-}) + (1 - x_{org})\Delta G^\circ_{hyd}(X^{m-}) \quad (11)$$

Introducing the midpoint potentials, $\Delta G^\circ_{excess}(X^{m-})$ can be determined as:

$$\Delta G^\circ_{excess}(X^{m-}) = \Delta G^\circ_{solv}(X^{m-}) - \Delta G^\circ_{solv}(X^{m-})*$$
$$= mF[(1 - x_{org})E_{mp}^w + x_{org}E_{mp}^s - E_{mp}^{mix}] \quad (12)$$

where E_{mp}^{mix} is the midpoint potential for the X^{m-}-assisted oxidation process in a binary solvent mixture having a molar fraction of organic solvent x_{org}.

The method is limited, however, in cases where the oxidized form of the complexes becomes soluble in a determined interval of composition of the solvent mixture, as previously noted. This can be seen in Figure 11 as the variation of SWV potentials on the molar fraction of MeOH for **L1**-modified graphite electrodes immersed into 0.10 M Na_3PO_4/(water + MeOH) mixtures.

The values of $\Delta G^\circ_{excess}(X^{m-})$ calculated from electrochemical data at **L2**-modified electrodes for perchlorate and acetate ions in MeOH + water and MeCN + water binary mixtures are shown in Figure 12. The obtained results are in agreement with recent modeling of Kashyap and Biswas[76] using the mean spherical approximation for solvent mixtures.

■ CONCLUSIONS

Upon attachment to graphite electrodes, the alkynyl-diphosphine dinuclear Au(I) complexes **L1** and **L2** and the heterometallic Au(I)−Cu(I) clusters **L3** and **L4** display essentially reversible ferrocenyl-localized solid-state oxidation processes. Such electrochemical processes involve the insertion of anions into the solid lattice, so that the voltammetric midpeak potentials are anion-dependent and exhibit a Nernstian-like variation with the concentration of the anion.

Voltammetric data can be used for a direct measurement of the individual Gibbs energy of anion transfer from one solvent to another from midpeak potentials in solutions of suitable salts in each one of the solvents separately or mixtures of the solvents. This methodology permits us to calculate the Gibbs free energy of ion transfer in cases where there is no disposal of soluble salts in a given solvent from polynomial variations of the midpeak potential with the molar fraction of organic solvent in water −MeOH and water−MeCN mixtures.

Voltammetric data can be used for determining the actual Gibbs energy of anion solvation in solvent mixtures and, combining such data with those for the pure solvents, the excess free energy of anion solvation in binary solvent mixtures. Combining the Gibbs energy of ion transfer with available Gibbs energies for ion hydration, the ΔG°_{solv} values for ions in different solvents can also be estimated. These results illustrate the inherent capabilities of the VMPs approach for obtaining thermochemical data.

■ AUTHOR INFORMATION

Corresponding Author
*E-mail: antonio.domenech@uv.es.

■ REFERENCES

(1) Conway, B. E. *Ionic Hydration in Chemistry and Biophysics*; Elsevier: New York, 1981.

(2) Marcus, Y. *Ion Solvation*; Wiley: New York, 1985.

(3) Rose, D.; Benjamin, I. Free Energy of Transfer of Hydrated Ion Clusters from Water to an Immiscible Organic Solvent. *J. Phys. Chem. B* **2009**, *113*, 9296–9303.

4584

dx.doi.org/10.1021/je200514c |*J. Chem. Eng. Data* 2011, 56, 4577–4586

(4) Kelly, C. P.; Cramer, C. J.; Truhlar, D. G. Free Energy of Transfer of Hydrated Ion Clusters from Water to an Immiscible Organic Solvent. *J. Phys. Chem. B* **2007**, *111*, 408–422.

(5) Tissandier, M. D.; Cowen, K. A.; Feng, W. Y.; Gundlach, E.; Cohen, M. H.; Earhart, A. D.; Coe, J. V. Free Energy of Transfer of Hydrated Ion Clusters from Water to an Immiscible Organic Solvent. *J. Phys. Chem. A* **1998**, *102*, 7787–7794.

(6) Tawa, G. J.; Topol, I. A.; Burk, S. K.; Rashin, A. A. Calculation of the aqueous solvation free energy of the proton. *J. Chem. Phys.* **1998**, *109*, 4852–4863.

(7) Pliego, J. R., Jr.; Riveros, J. M. Ions in a binary asymmetric dipolar mixture: Mole fraction dependent Born energy of solvation and partial solvent polarization structure. *Phys. Chem. Chem. Phys.* **2002**, *4*, 1622–1627.

(8) Topol, I. A.; Tawa, G. J.; Burk, S. K.; Caldwell, R. A.; Rashin, A. A. On the structure and thermodynamics of solvated monoatomic ions using a hybrid solvation model. *J. Chem. Phys.* **1999**, *111*, 10998–11014.

(9) Mejias, J. A.; Lago, S. Calculation of the absolute hydration enthalpy and free energy of H^+ and OH^-. *J. Chem. Phys.* **2000**, *113*, 7306–7316.

(10) Zhan, C.-G.; Dixon, D. A. Hydration of the Fluoride Anion: Structures and Absolute Hydration Free Energy from First-Principles Electronic Structure Calculations. *J. Phys. Chem. A* **2004**, *108*, 2020–2029.

(11) Zhan, C.-G.; Dixon, D. A. Absolute Hydration Free Energy of the Proton from First-Principles Electronic Structure Calculations. *J. Phys. Chem. A* **2001**, *105*, 11534–11540.

(12) Zheng, F.; Zhan, C.-G.; Ornstein, R. L. Theoretical Determination of Two Structural Forms of the Active Site in Cadmium-Containing Phosphotriesterases. *J. Phys. Chem. B* **2002**, *106*, 717–722.

(13) Zhan, C.-G.; Dixon, D. A.; Sabri, M. I.; Kim, M.-S.; Spencer, P. S. Theoretical Determination of Chromophores in the Chromogenic Effects of Aromatic Neurotoxicants. *J. Am. Chem. Soc.* **2002**, *124*, 2744–2752.

(14) Ahlquist, M.; Kozuch, S.; Shaik, S.; Tanner, D.; Norrby, P.-O. On the Performance of Continuum Solvation Models for the Solvation Energy of Small Anions. *Organometallics* **2006**, *25*, 45–47.

(15) Samec, Z. Electrochemistry at the interface between two immiscible electrolyte solutions. *Pure Appl. Chem.* **2004**, *76*, 2147–2180.

(16) Dryfe, R. A. W. Gibbs energy of solvation of organic ions in aqueous and dimethyl sulfoxide solutions. *Phys. Chem. Chem. Phys.* **2006**, *8*, 1869–1883.

(17) Langmaier, J.; Samec, Z. Cyclic voltammetry of ion transfer across a room temperature ionic liquid membrane supported by a microporous filter. *Electrochem. Commun.* **2007**, *9*, 2633–2638.

(18) Sherburn, A.; Platt, M.; Arrigan, D. W. M.; Boag, N. M.; Dryfe, R. A. W. Selective silver ion transfer voltammetry at the polarised liquid| liquid interface. *Analyst* **2003**, *128*, 1187–1192.

(19) Josserand, J.; Lagger, G.; Jensen, H.; Ferrigno, R.; Girault, H. H. Contact Galvani potential differences at liquid—liquid interfaces: Part II. Contact diffusion potentials in microsystems. *J. Electroanal. Chem.* **2003**, *546*, 1–13.

(20) Sun, P.; Laforge, F. O.; Mirkin, M. V. Modifying the liquid/ liquid interface: pores, particles and deposition. *Phys. Chem. Chem. Phys.* **2007**, *9*, 802–823.

(21) Sun, P.; Laforge, F. O.; Mirkin, M. V. Role of Trace Amounts of Water in Transfers of Hydrophilic and Hydrophobic Ions to Low-Polarity Organic Solvents. *J. Am. Chem. Soc.* **2007**, *129*, 12410–12411.

(22) Olaya, A. J.; Méndez, M. A.; Cortes-Salazar, F.; Girault, H. H. Voltammetric determination of extreme standard Gibbs ion transfer energy. *J. Electroanal. Chem.* **2010**, *644*, 60–66.

(23) Gulaboski, R.; Scholz, F. Lipophilicity of Peptide Anions: An Experimental Data Set for Lipophilicity Calculations. *J. Phys. Chem. B* **2003**, *107*, 5650–5657.

(24) Scholz, F. Recent advances in the electrochemistry of ion transfer processes at liquid—liquid interfaces. *Annu. Rep. Prog. Chem. Sect. C* **2006**, *102*, 43–70.

(25) Marken, F.; McKenzie, K. J.; Shul, G.; Opallo, M. Ion transfer processes at 4-(3-phenylpropyl)-pyridine | aqueous electrolyte | electrode triple phase boundary systems supported by graphite and by mesoporous TiO_2. *Faraday Discuss.* **2005**, *129*, 219–229.

(26) MacDonald, S. M.; Opallo, M.; Klamt, A.; Eckert, F.; Marken, F. Scanning electrochemical microscopy in the 21st century. *Phys. Chem. Chem. Phys.* **2008**, *10*, 3925–3933.

(27) Donald, A. W.; Leib, R. D.; O'Brien, J. T.; Bush, M. F.; Williams, E. R. Absolute Standard Hydrogen Electrode Potential Measured by Reduction of Aqueous Nanodrops in the Gas Phase. *J. Am. Chem. Soc.* **2008**, *130*, 3371–3381.

(28) Cox, B. G.; Parker, A. J.; Waghorne, W. E. Liquid junction potentials between electrolyte solution in different solvents. *J. Am. Chem. Soc.* **1973**, *95*, 1010–1014.

(29) Bjerrum, N.; Larsson, E. Studien über Ionenverteilungskoeffizienten. *Z. Phys. Chem.* **1927**, *127*, 358.

(30) Alexander, R.; Parker, A. Solvation of ions. XII. Changes in the standard chemical potential of anions on transfer from protic to dipolar aprotic solvents. *J. Am. Chem. Soc.* **1967**, *89*, 5549–5551.

(31) Popovych, O.; Dill, A. J. Single scale for ion activities and electrode potentials in ethanol-water solvents based on the triisoamyl-butylammonium tetraphenylborate assumption. *Anal. Chem.* **1969**, *41*, 456–462.

(32) Strehlow, H.; Schneider, H. Solvation of ions in pure and mixed solvents. *Pure Appl. Chem.* **1971**, *25*, 327–344.

(33) Gritzner, G. Gibbs free energies of transfer (ΔG_{tr}) for alkali metal ions and tl^+. *Inorg. Chim. Acta* **1977**, *24*, 5–12.

(34) Gritzner, G.; Kuta, J. Recommendations on reporting electrode potentials in nonaqueous solvents. *Pure Appl. Chem.* **1984**, *56*, 461–466.

(35) Gritzner, G. Polarographic half-wave potentials of cations in nonaqueous solvents. *Pure Appl. Chem.* **1990**, *62*, 1839–1858.

(36) Gritzner, G. Single-ion transfer properties: a measure of ion-solvation in solvents and solvent mixtures. *Electrochim. Acta* **1998**, *44*, 73–83.

(37) Koshevoy, I. O.; Smirnova, E. S.; Doménech, A.; Karttunen, A. J.; Haukka, M.; Tunik, S. P.; Pakkanen, T. A. Synthesis, electrochemical and theoretical studies of the Au(I)-Cu(I) heterometallic clusters bearing ferrocenylgroups. *Dalton Trans.* **2009**, 8392–8398.

(38) Koshevoy, I. O.; Koskinen, L.; Haukka, M.; Tunik, S. P.; Serdobintsev, P. Y.; Melnikov, A. S.; Pakkanen, T. A. Self-assembly of Supramolecular Luminescent Gold(I)-Copper(I) Complexes: "Wrapping" the Au_6Cu_6 Cluster with $[Au_3(diphosphine)_3]^{3+}$ Belt. *Angew. Chem., Int. Ed.* **2008**, *47*, 3942–3945.

(39) Koshevoy, I. O.; Karttunen, A. J.; Tunik, S. P.; Haukka, M.; Selivanov, S. I.; Melnikov, A. S.; Serdobintsev, P. Y.; Khodorkovskiy, M. A.; Pakkanen, T. A. Supramolecular Luminescent Gold(I)—Copper-(I) Complexes: Self-Assembly of the AuxCuy Clusters inside the $[Au3(diphosphine)_3]^{3+}$ Triangles. *Inorg. Chem.* **2008**, *47*, 9478–9488.

(40) Koshevoy, I. O.; Karttunen, A. J.; Tunik, S. P.; Haukka, M.; Selivanov, S. I.; Melnikov, A. S.; Serdobintsev, P. Y.; Pakkanen, T. A. Synthesis, Characterization, Photophysical, and Theoretical Studies of Supramolecular Gold(I)—Silver(I) Alkynyl-Phosphine Complexes. *Organometallics* **2009**, *28*, 1369–1376.

(41) Koshevoy, I. O.; Lin, Y.-C.; Karttunen, A. J.; Pakkanen, T. A. Intensely Luminescent Alkynyl—Phosphine Gold(I)—Copper(I) Complexes: Synthesis, Characterization, Photophysical, and Computational Studies. *Inorg. Chem.* **2009**, *48*, 2094–2102.

(42) Scholz, F.; Meyer, B. In *Electroanalytical Chemistry, A Series of Advances*; Bard, A. J., Rubinstein, I., Eds.; Marcel Dekker: New York, 1998; Vol. 20, pp 1–86.

(43) Scholz, F.; Schröder, U.; Gulaboski, R. *Electrochemistry of Immobilized Particles and Droplets*; Springer: Berlin-Heidelberg, 2005.

(44) Doménech, A.; Koshevoy, I. O.; Montoya, N.; Pakkanen, T. A. Electrochemically assisted anion insertion in Au(I)—Cu(I) heterotri-metallic clusters bearing ferrocenyl groups: Application to the fluoride/ chloride discrimination in aqueous media. *Electrochem. Commun.* **2010**, *12*, 206–209.

(45) Wooster, T. J.; Bond, A. M.; Honeychurch, M. J. An Analogy of an Ion-Selective Electrode Sensor Based on the Voltammetry of Microcrystals of Tetracyanoquinodimethane or Tetrathiafulvalene Adhered to an Electrode Surface. *Anal. Chem.* **2003**, *75*, 586–592.

(46) Wooster, T. J.; Bond, A. M. Ion selectivity obtained under voltammetric conditions when a TCNQ chemically modified electrode is presented with aqueous solutions containing tetraalkylammonium cations. *Analyst* **2003**, *128*, 1386–1390.

(47) Doménech, A.; Koshevoy, I. O.; Montoya, N.; Pakkanen, T. A. Electrochemical anion sensing using electrodes chemically modified with Au(I)-Cu(I) heterotrimetallic alkynyl cluster complexes containing ferrocenyl groups. *Anal. Bioanal. Chem.* **2010**, *397*, 2013–2022.

(48) Doménech, A.; Koshevoy, I. O.; Montoya, N.; Pakkanen, T. A. Estimation of free energies of anion transfer from solid-state electrochemistry of alkynyl-based Au(I) dinuclear and Au(I)−Cu(I) cluster complexes containing ferrocenyl groups. *Electrochem. Commun.* **2011**, *13*, 96–98.

(49) Doménech, A.; Montoya, N.; Scholz, F. Estimation of individual Gibbs energies of cation transfer employing the insertion electrochemistry of solid Prussian blue. *J. Electroanal. Chem.* **2011**, *657*, 117–122.

(50) Gulaboski, R.; Caban, K.; Stojek, Z.; Scholz, F. The determination of the standard Gibbs energies of ion transfer between water and heavy water by using the three-phase electrode approach. *Electrochem. Commun.* **2004**, *6*, 215–218.

(51) Moore, R. R.; Banks, C. E.; Compton, R. G. Basal Plane Pyrolytic Graphite Modified Electrodes: Comparison of Carbon Nanotubes and Graphite Powder as Electrocatalysts. *Anal. Chem.* **2004**, *76*, 2677–2682.

(52) Becke, A. D. Density-functional exchange-energy approximation with correct asymptotic behaviour. *Phys. Rev. A* **1988**, 3098–3100.

(53) Weigend, F.; Ahlrichs, R. Probing carboxylate Gibbs transfer energies via liquid−liquid transfer at triple phase boundary electrodes: ion-transfer voltammetryversus COSMO-RS predictions. *Phys. Chem. Chem. Phys.* **2005**, *7*, 3297–3305.

(54) Andrae, D.; Häussermann, U.; Dolg, M.; Stoll, H.; Preuss, H. Energy-adjusted *ab initio* pseudopotentials for the second and third row transition elements. *Theor. Chem. Acc.* **1990**, *77*, 123–141.

(55) Schäfer, A.; Horn, H.; Ahlrichs, R. Fully optimized contracted Gaussian basis sets for atoms Li to Kr. *J. Chem. Phys.* **1992**, *97*, 2571–2577.

(56) Weigend, F. Accurate Coulomb-fitting basis sets for H to Rn. *Phys. Chem. Chem. Phys.* **2006**, *8*, 1057–1065.

(57) Ahlrichs, R.; Bär, M.; Häser, M.; Horn, H.; Kölmel, C. The lowest triplet state of a diacetylene. *Chem. Phys. Lett.* **1989**, *62*, 165–169.

(58) Bond, A. M.; Fletcher, S.; Marken, F.; Shaw, S. J.; Symons, P. J. Electrochemical and X-ray diffraction study of the redox cycling of nanocrystals of 7,7,8,8-tetracyanoquinodimethane. Observation of a solid−solid phase transformation controlled by nucleation and growth. *J. Chem. Soc., Faraday Trans.* **1996**, *92*, 3925–3933.

(59) Lovric, M.; Scholz, F. A model for the propagation of a redox reaction through microcrystals. *J. Solid State Electrochem.* **1997**, *1*, 108–113.

(60) Lovric, M.; Hermes, M.; Scholz, F. The effect of the electrolyte concentration in the solution on the voltammetric response of insertion electrodes. *J. Solid State Electrochem.* **1998**, *2*, 401–404.

(61) Oldham, K. B. Voltammetry at a three-phase junction. *J. Solid State Electrochem.* **1998**, *2*, 367–377.

(62) Lovric, M.; Scholz, F. A model for the coupled transport of ions and electrons in redox conductive microcrystals. *J. Solid State Electrochem.* **1999**, *3*, 172–175.

(63) Schröder, U.; Oldham, K. B.; Myland, J. C.; Mahon, P. J.; Scholz, F. Modelling of solid state voltammetry of immobilized microcrystals assuming an initiation of the electrochemical reaction at a three-phase junction. *J. Solid State Electrochem.* **2000**, *4*, 314–324.

(64) Rajagopal, A.; Wu, C. I.; Kahn, A. Energy level offset at organic semiconductor heterojunctions. *J. Appl. Phys.* **1998**, *83*, 2649.

(65) Tsiper, E. V.; Soos, Z. G.; Gao, W.; Kahn, A. Electronic polarization at surfaces and thin films of organic molecular crystals: PTCDA. *Chem. Phys. Lett.* **2002**, *360*, 47–52.

(66) D'Andrade, B. W.; Datta, S.; Forrest, S. R.; Djurovich, P.; Polikarpov, E.; Thompson, M. E. Relationship between the ionization and oxidation potentials of molecular organic semiconductors. *Org. Electron.* **2005**, *6*, 11–20.

(67) Cox, B. G.; Waghorne, W. E. Thermodynamics of ion-solvent interactions. *Chem. Soc. Rev.* **1980**, *9*, 381–411.

(68) Moyer, S. A.; Bonnesen, P. V. In *Supramolecular Chemistry of Anions*; Bianchi, A., García-España, E., Bowman-James, K., Eds.; Wiley: New York, 1997; pp 1−44.

(69) Johnsson, M.; Persson, I. Determination of Gibbs free energy of transfer for some univalent ions from water to methanol, acetonitrile, dimethylsulfoxide, pyridine, tetrahydrothiophene and liquid ammonia; standard electrode potentials of some couples in these solvents. *Inorg. Chim. Acta* **1987**, *127*, 15–24.

(70) Marcus, Y.; Kamlet, M. J.; Taft, R. W. Linear solvation energy relationships: standard molar Gibbs free energies and enthalpies of transfer of ions from water into nonaqueous solvents. *J. Phys. Chem.* **1988**, *92*, 3613–3622.

(71) Marcus, Y. Thermodynamics of solvation of ions. Part 5.—Gibbs free energy of hydration at 298.15 K. *J. Chem. Soc., Faraday Trans.* **1991**, *87*, 2995–2999.

(72) Francesconi, R.; Comelli, F. Excess molar enthalpies of binary mixtures containing dialkylcarbonates + cyclic ketones at 298.15 or 313.15 K. *Thermochim. Acta* **1995**, *258*, 49–57.

(73) Marcus, Y. *Solvent Mixtures: Properties and Selective Solvation*; CRC Press: Boca Raton, FL, 2002.

(74) Yamazaki, T.; Kovalenko, A.; Murashov, V. V.; Patey, G. N. Ion Solvation in a Water−Urea Mixture. *J. Phys. Chem. B* **2010**, *114*, 613–619.

(75) Gulaboski, R.; Mircesky, V.; Lovric, M.; Bogeski, I. Theoretical study of a surface electrode reaction preceded by a homogeneous chemical reaction under conditions of square-wave voltammetry. *Electrochem. Commun.* **2005**, *7*, 515–522.

(76) Kashyap, H. K.; Biswas, R. Ions in a binary asymmetric dipolar mixture: Mole fraction dependent Born energy of solvation and partial solvent polarization structure. *J. Chem. Phys.* **2007**, *127*, 184502.